Next Nanotechnology 7 (2025) 100103

Contents lists available at ScienceDirect

Next Nanotechnology

journal homepage: www.sciencedirect.com/journal/next-nanotechnology

Surface treatments with TiO_2 nanostructures for bonding to zirconia materials as an alternative to conventional airborne-particle abrasion of the surface

Constantino Fernandes-Neto [a], Erika Bronze-Uhle [a], Leonardo Francisco Gonçalves Dias [b], Fabio Antonio Piola Rizzante [c], Paulo Noronha Lisboa-Filho [d], Adilson Yoshio Furuse [a,*]

[a] Department of Operative Dentistry, Endodontics and Dental Materials, Bauru School of Dentistry, University of São Paulo, Bauru, SP 17012-901, Brazil
[b] Physicochimie des Eletrolytes et Nanosystèmes Interfaciaux (PHENIX), Sorbonne Université, CNRS, Paris, France
[c] Department of Oral Rehabilitation, James B. Edwards College of Dental Medicine, Medical University of South Carolina, Charleston, SC, USA
[d] Professor, Department of Physics, School of Science, UNESP – São Paulo State University, Bauru, SP, Brazil

ARTICLE INFO

Keywords:
Ceramics
Y-TZP ceramic
Titanium dioxide
Nanotubes
Shear strength

ABSTRACT

Zirconia has become a popular choice for indirect restorations; however, adhesion to this material remains a challenge. The present study aimed to evaluate surface characteristics and bond strength to tetragonal Y-TZP and cubic Y-PSZ zirconia submitted to experimental surface treatments. Specimens of Y-TZP (T) and Y-PSZ (P) were prepared and divided into groups: Tf-A) thin TiO_2 film functionalized with 3-(aminopropyl)trimethoxysilane (APTMS); Tf) thin TiO_2 film; MNt-A) manual application of TiO_2 nanotubes with APTMS; MNt) manual application of TiO_2 nanotubes; VNt-A) vacuum application of TiO_2 nanotubes with APTMS; VNt) vacuum application of TiO_2 nanotubes; C) control with Al_2O_3 sandblasting. Characterization with x-ray photoelectron spectroscopy (XPS) and scanning electron microscopy (SEM) was done. Bond strength was evaluated by microshear bond strength (μSBS). Data were analyzed by two-way ANOVA and Tukey's HSD tests ($\alpha = 0.05$). XPS showed signals for elements O 1 s, Ti 2p, and Zr 3d 5/2. In addition, high-resolution demonstrated Ti-O-Si and Zr-O-Si bonding for treatments with TiO_2 and APTMS for T-Tf-A/P-Tf-A. SEM presented a homogeneous film for T-Tf/T-Tf-A/P-Tf/P-Tf-A and cluster formations for all nanotube groups. Control groups for both Y-TZP and Y-PSZ showed clear surfaces. No differences of μSBS were seen between experimental surface treatments and the controls, except for T-MNt-A/T-VNt-A/P-MNt-A/P-VNt-A, which showed the lowest mean μSBS and highest incidence of pre-test failures. Surface treatments with TiO_2 nanostructures were effective in modifying the surface of both zirconia materials evaluated, providing strong covalent bonds, changes to the surface topology, and shear bond strength comparable to conventional sandblasting protocols.

1. Introduction

Zirconia materials are known for their excellent physical, mechanical and thermal properties, as well as their high biocompatibility [1]. Among several compositions of zirconia, yttria-stabilized tetragonal zirconia polycrystals (Y-TZP) are classically used for cores and monolithic crowns, while zirconia partially stabilized by yttria (Y-PSZ) are indicated for esthetic monolithic restorations [2]. However, its dense polycrystalline structure results in an inert surface, which hinders bonding to resin-based materials [3]. It is known that all-ceramic dental restorations, such as veneers and onlays, depend inherently on resin cements. For that matter, Y-TZP and Y-PSZ cannot be etched with hydrofluoric acid followed by application of a silane coupling agent, since these ceramics do not present silica or glassy phase on their structures, impeding the acid etch that would be responsible for providing micromechanical interlocking [4–6]. As a result, alternative techniques were proposed to modify the surface of zirconia [7–12], which include mainly combining sandblasting followed by the application of an adhesive [13,14]. Nonetheless, a consensus has not been reached as to which is the protocol of treatment [14]. Furthermore, sandblasting is not always the

* Correspondence to: Department of Operative Dentistry, Endodontics and Dental Materials, Bauru School of Dentistry, University of São Paulo, Alameda Dr. Octávio Pinheiro Brisolla, 9-75, Bauru, SP CEP 17012-901, Brazil.
E-mail address: furuse@usp.br (A.Y. Furuse).

https://doi.org/10.1016/j.nxnano.2024.100103
Received 16 September 2023; Received in revised form 16 August 2024; Accepted 4 September 2024
Available online 16 September 2024

most recommended treatment as it can lead to formation of microcracks in the surface of the material [15], and it might be harmful to cubic phase zirconia materials, which are not able to impair crack propagation by martensitic transformation [16].

An alternative method would be coating the surface by non-mechanical methods. In this sense, the use of nanotechnology to modify the surface of zirconia with metallic oxides to improve bonding has been studied [17,18]. Dos Santos et al. [17] demonstrated an interesting method of incorporation of titanium dioxide (TiO_2) nanotubes over the surface of pre-sintered Y-TZP. TiO_2 nanotubes present a small size and high density of surface sites [19], which increase surface free energy and facilitate posterior application of luting agents [20]. Although the study by Dos Santos suggests advantages for the functionalization of the ceramic surface, further investigation is needed to validate such hypotheses and elaborate on the forms of application of TiO_2 structures [17,21,22]. Another approach recently proposed is the application of TiO_2 nanotubes by using vacuum [23]. This method consists of immersing the zirconia in a solution of TiO_2 nanotubes and applying vacuum to it [23].

TiO_2 is an extensively studied metallic oxide with interesting optical [24], photocatalytic [25], anticorrosive [26], and antimicrobial properties [27]. It may be presented in the crystalline forms of rutilo and anatase, among other forms. Anatase requires lower temperatures for its transformation and has shown antimicrobial properties, while rutilo phase is more stable and requires higher temperatures for its transformation [28,29]. In addition, the surface of TiO_2 is mainly terminated with groups hydroxyl (-OH), which can be promptly functionalized with various bifunctional molecules, such as siloxanes [30,31]. As a result of functionalization, covalent bonds are formed with metals through reactions in the surface with hydroxyl groups [30,31]. The functionalization of ceramic surfaces with TiO_2 nanostructures is already used to provide bioactivity to it, becoming self-cleaning and antimicrobial [28,32,33]. Studies also have shown that such application was effective in altering the surface of zirconium oxide specimens, favoring the posterior step of silanization [24,34]. Besides, the formation of interatomic bonds of high energy between TiO_2 and siloxanes allow them to be functionalized and further present good interaction with resin-based luting agents [35]. In addition to these properties, the photocatalytic property of TiO_2 also increases its surface free energy and facilitates the application of luting agents [20]. Therefore, the evaluation of surface treatments with TiO_2 over zirconia surfaces may provide effective and even improved bonding to Y-TZP and Y-PSZ without harming the ceramic structure.

In this context, the aim of the present study was to evaluate surface characteristics and bond strength of Y-TZP and Y-PSZ to a resin-cement after surface treatments with the growth of TiO_2 thin films or application of TiO_2 nanotubes (manually or in vacuum), as compared to conventional sandblasting with Al_2O_3. The functionalization with 3-(aminopropyl)trimethoxysilane (APTMS) was also evaluated. Surfaces treated with experimental treatments were characterized through XPS and SEM. Bond strength evaluation was performed using a commercially available resin cement. Thus, the null hypothesis was that, (1) surface treatments with TiO_2 structures would not modify the surfaces of zirconia materials; in regards to bond strength, there would be (2) no differences between zirconia materials, and (3) no differences between surface treatments.

2. Material and methods

The trade name, lot, chemical composition, and manufacturers of the employed materials used in the present study are listed in Table 1. Y-TZP and Y-PSZ were cut in slices of 1.7 mm in a cutting machine (Isomet 1000 Low Speed Saw, Buehler, LakeBluff) with diamond disk (Wafer Blade, 5-inch x 0.15-inch x 0.15-inch) at a speed of 275 rpm and constant water-cooling. Slices were polished with a sequence of silicon carbide sandpaper (#800, #1200, K2000 Polishing Paper, Exact) in a metallographic polishing machine (Exact) under constant water-cooling. Specimens presented a final dimension of 7.5 ×5.0 mm×1.5 mm.

Table 1
Brand name, manufacturer and composition of materials used in the study.

Trade name	Manufacture	Composition	Lot
IPS e-max ZirCAD	Ivoclar Vivadent, AG, Schaan, Liechtentein	Zirconium oxide, yttrium oxide, hafnium oxide, aluminium, other oxides	S17366
IPS e-max ZirCAD MT	Ivoclar Vivadent, AG, Schaan, Liechtentein	Zirconium oxide, yttrium oxide, hafnium oxide, aluminium, other oxides	W31929
Aluminum oxide	Polidental, Cotia, Brazil	Aluminum oxide (150 μm)	16758
Monobond-N	Ivoclar Vivadent, AG, Schaan, Liechtentein	Ethanol, silane methacrylate, phosphoric acid methacrylate, and sulphide methacrylate.	Y43736
Multilink N Primer A	Ivoclar Vivadent, AG, Schaan, Liechtentein	Water, initiators.	Y37839
Multilink N Primer B	Ivoclar Vivadent, AG, Schaan, Liechtentein	Phosphoric acid acrylate, hydroxyethyl methacrylate, Methacrylate modified polyacrylic acid, stabilizers.	Y41401
Multilink N	Ivoclar Vivadent, AG, Schaan, Liechtentein	Dimethacrylate and HEMA, Barium glas filler and silicon dioxide filler, yttriumtrfluoride, catalysts and stabilizer, pigments	Y30903
APTMS	Sigma-Aldrich, Darmstadt, HE, Germany	3-(aminopropyl) trimethoxysilane 97 % assay.	BCBV6395

HEMA – 2-hydroxyethyl methacrylate.

Zirconia slices were divided into 14 groups (n=10), varying the material (in 2 levels), surface treatment and functionalization method (7 levels), according to Table 2. Samples of Y-TZP and Y-PSZ were divided according to surface treatments, being treated with TiO_2 thin film– Tf; Manual application of TiO_2 nanotubes on pre-sintered ceramics – MNt; Vacuum application of TiO_2 nanotubes on pre-sintered ceramics – VNt; Control – C. Samples were also labeled for the functionalization method with 3-(aminopropyl)trimethoxysilane (APTMS) (A). Prior to cementation, control groups were sandblasted with 100 μm aluminum oxide. All materials described in Table 1 were used as per manufacturers' instructions.

For the treatment with thin film deposition, a TiO_2 solution was synthesized by a sol-gel route, through hydrolysis and condensation reaction of titanium isopropoxide (IV). The synthesis used a high molar ratio of water: alcoxide (200:1) and included isopropanol as co-solvent, nitric acid (HNO_3) as a catalyst and Triton X-100 as a surfactant. Distilled water (185 mL), isopropanol (56.7 mL, Merck), nitric acid (2.6 mL, Synth), and titanium isopropoxide (IV) (15 mL, Aldrich) were mixed and stirred for 30 min. The reaction beaker was covered, and the

Table 2
Groups according to material and surface treatment.

Material	Surface treatment	Acronym
Y-TZP	TiO_2 thin film with APTMS	T-Tf-A
	TiO_2 thin film with Monobond N*	T-Tf
	Manual nanotubes with APTMS	T-MNt-A
	Manual nanotubes with Monobond N*	T-MNt
	Vacuum nanotubes with APTMS	T-VNt-A
	Vacuum nanotubes with Monobond N*	T-VNt
	Control with Al_2O_3 sandblast and Monobond N*	T-C
Y-PSZ	TiO_2 thin film with APTMS	P-Tf-A
	TiO_2 thin film with Monobond N*	P-Tf
	Manual nanotubes with APTMS	P-MNt-A
	Manual nanotubes with Monobond N*	P-MNt
	Vacuum nanotubes with APTMS	P-VNt-A
	Vacuum nanotubes with Monobond N*	P-VNt
	Control with Al_2O_3 sandblast and Monobond N*	P-C

*Monobond N application and Al2O3 sandblast were only used for μSBS.

solution was heated at 85 ºC under magnetic stirring for 4 h to allow peptization. At this stage, solvents were evaporated during hydrolysis, leading to the condensation of colloids of light translucent blue color. Aiming to form a gel phase, the solution was heated and stirred until 50 mL of volume remained, presenting a milky-white color. Ultimately, Triton X-100 surfactant (0.816 g, Synth) was poured and stirred for 15 min [31]. The deposition was performed with a spin coater (PWM32-OS-R790, Headway Research INC), the liquid was applied over the surface and submitted to a rotation of 2000 rpm for 60 s. Subsequently, samples were heated to 850ºC for 2 h at a rate of 1 ºC/min to obtain rutile crystalline phase. Specimens were submitted to UV-light during 10 minutes in a chamber mounted using a 15 W UV-light (Philips 15 W, peak wavelengths of 365 and 254 nm), following previous protocol [36].

For treatments with TiO_2 nanotubes, the nanostructure was synthesized through an alkaline hydrothermal process. In a teflon container, twelve grams of TiO_2 anatase powder (99 %, Aldrich) were mixed with 120 mL of NaOH solution (10 M) and kept at 120°C for 24 h, in a glycerin bath at ambient atmospheric pressure. After 24 h of alkaline treatment, the TiO_2 solution was washed and centrifuged with deionized water and hydrochloric acid (HCl) solution (0.1 M) until the pH of the solution reached 4.0. The pasty material obtained was subjected to a drying process at 200 °C for 24 h using a heating/cooling rate of 10 °C/min.

The manual application was performed by preparing a solution of 17.5 mL of 100 % alcohol and 0.292 g of TiO_2 nanotube powder, which was mechanically prepared using a vortex mixer (K45–2820, Kasvi) at 2800 rpm and 60 Hz. The solution was manually applied over presintered zirconia surfaces with a microbrush. Alcohol was then evaporated with oil-free air jet with a pressure of 40 psi, applied at 45° from 10 cm distance for 10 s.

Vacuum application was carried out by placing the presintered zirconia slices inside a Büchner flask with the same solution of TiO_2 nanotubes previously prepared. High-pressure vacuum infiltration was applied for 5 min at 70 kPa with a compressor (DIA-PUMP 089/C; FANEM).

Following surface treatments, samples were silanized by immersion in a solution of 3 mM of APTMS (Sigma-Aldrich, Hamburg, Germany), which was prepared in HPLC ethanol and stirred for 5 min in a magnetic plate. After complete dissolution, the samples were immersed for 1 h at room temperature (25 ºC) and atmospheric pressure. Subsequently, samples were immersed and agitated in ethanol three times to remove adsorbed molecules.

2.1. X-ray photoelectron spectroscopy (XPS)

X-ray photoelectron spectroscopy was performed for samples treated with TiO_2 and APTMS silanization, using a conventional spectrophotometer (ESCA +, Scientia Omicron). The analysis was done with 128-channel hemispherical analyzer (EAC-2000), equipped with a micro-focused Al Kα monochromator with variable aperture (30–400 μm adjustable every 5 μm) and incident energy of 1486.60 eV. XPS spectra were recorded at constant pass energy of 20 eV with 0.05 eV per step. All photoelectron spectra were calibrated using the C1s binding energy peak centered at 285 eV. CasaXPS (v2.3.18, Casa Software Ltd) was used to perform the peak energy and curve fitting analysis. Peak identification was performed to obtain a consistent combination of investigated potentials. OriginLab program (version 12.1, OriginLab Corporation) was used to generate graphs showing the peaks with the compounds and bindings of interest [31,36,37].

2.2. Scanning electron microscopy (SEM)

Samples were metallized with palladium-gold alloy followed by capture of the images of the surface by SEM (JSM, 220 A, JEOL, Tokyo, Japan), set at 10 kV accelerating voltage under vacuum. Five images per sample were taken at different magnifications and representative areas at 1000x magnification were chosen to compare groups.

2.3. Microshear bond strength (μSBS)

μSBS evaluation was performed after the cementation of ø1.4 mm resin composite cylinders (Z350XT A2B, 3 M ESPE) over the samples. Cementation procedures were conducted with the resin cement Multilink N (Table 1). Control groups were sandblasted with aluminum oxide 100 μm at a pressure of 0.28 MPa, distance of 10 mm, and angle of 45º for 10 s, using a sandblaster (Basic Master, Renfert). Monobond N was applied in all groups, except on the ones in which APTMS was used, following the manufacturer's instruction. Multilink N was applied at one side of the cylinder, which was stabilized, excess was removed, and curing was performed with a LED curing unit (Radii-cal, SDI) positioned beneath the ceramic, according to previous studies [38]. Specimens were submitted to artificial aging by thermocycling in deionized water for 10,000 cycles at 5ºC and 55ºC water baths (Thermocycle; BioPDI) with a dwell time of 15 s. The μSBS was evaluated in a universal testing machine (Instron 3342, Illinois Tool Works), employing a 0.2 mm wire loop and a 500 N-load cell at a crosshead speed of 0.5 mm/min.

μSBS data was submitted to the Kolmogorov-Smirnov test of normality. Data were then analyzed with two-way ANOVA, considering zirconia materials and surface treatments as independent variables, and Tukey's HSD tests. A global level of significance of 5 % was adopted.

3. Results

Survey spectra results revealed the presence of the atoms of Zr 3d5/2 (182.30 eV) and O 1 s (530.00 eV) for all surface treatments on both Y-TZP and Y-PSZ, referring to pristine ZrO_2 (Figs. 1, 2). The substrates T-Tf, T-MNt, T-VNt and the same for the Y-PSZ groups, showed the signal referent to Ti 2p1/2 (458.75 eV) and the presence of TiO_2 on the surface. Si 2p (102.49 eV) and N 1 s (401.90 eV) were not detected in the survey spectra but were detected in the high-resolution spectra. Adventitious carbon C1s (285.00 eV) was detected and was used as a reference for the fitting curves. High resolution spectra were evaluated to determine the chemical and conformation binding of the compounds with their respective substrates (Fig. 3, 4, 5).

Figs. 3A and 3 C show Zr 3d and O 1 s high resolution spectra for both Y-TZP and Y-PSZ control groups. Zr 3d spectrum presents a doublet, as a consequence of spin orbital coupling, corresponding to Zr 3d 5/2 and Zr 3d 3/2. The peaks have binding energies around 181.5 eV/183.70 eV and 182.20 eV/184.62 eV for Y-TZP and Y-PSZ, respectively, and are identified as Zr^{4+} present on ZrO_2 [39–41]. The O

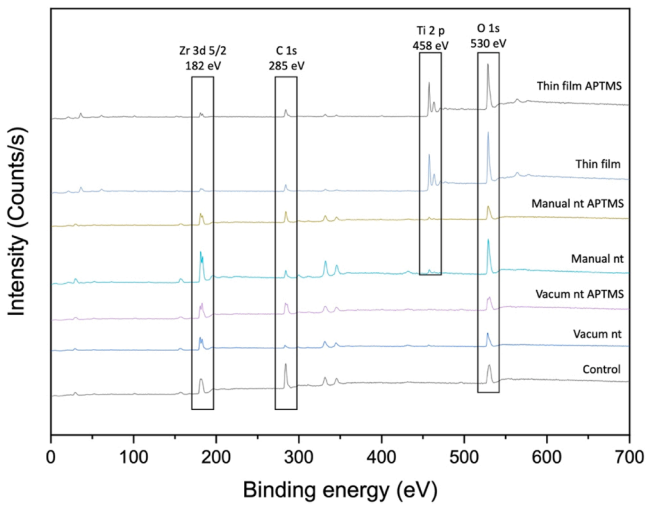

Fig. 1. Survey spectra from XPS analysis of Y-TZP obtained through CasaXPS (Casa Software Ltd) and Origin (EA).

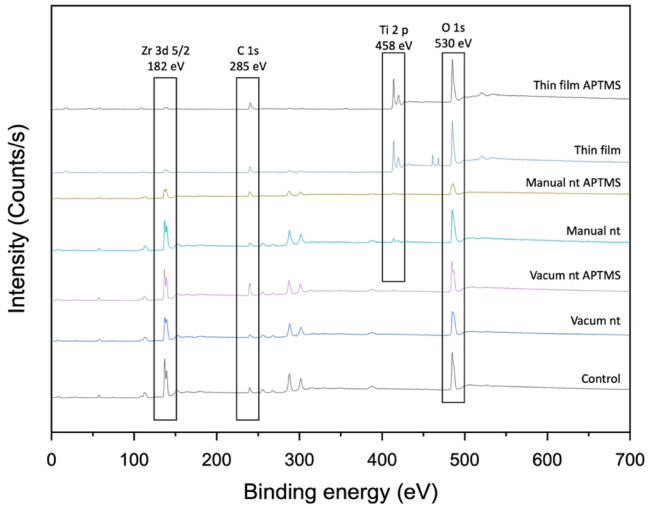

Fig. 2. Survey spectra from XPS analysis of Y-PSZ obtained through CasaXPS (Casa Software Ltd) and Origin (EA).

1 s deconvolution spectrum shows a main peak located at 531.00 eV for Y-TZP and two deconvolution peaks located at 530.20 eV (main peak) and 532.20 eV for Y-PSZ (Figs. 3B and 3D). Ti 2p high resolution spectra for T-Tf, T-MNt, T-VNt, P-Tf, P-MNt, P-VNt are displayed in Fig. 4. Ti 2p spectrum presents two spin orbit coupling contributions, Ti 2p1/2 and Ti 2p3/2 in 458.8± 0.2 eV and 464.6 ±0.2 eV, which are consistent to Ti^{4+} in TiO_2 bond (Ti-O bond) [42–44]. Fig. 5 presents high-resolution spectra of Si 2p and N1s for both Y-TZP and Y-PSZ. Si 2p spectrum shows a peak in the region of 102.40 eV, referring to Si-O-Ti/Si-O-bonds. T-VNt-A, presented Si 2p with two deconvolution peaks in the regions of 102.10 eV and 104.2 eV associated with of Si-O groups and SiO_2, respectively. N1s spectra for APTMS derivatives show, in general, curve fits with one or two components at binding energies in the region of 399.8 ± 0.5 eV - 401.5 ± 0.5 eV [45]. The N 1 s peak at low binding energy, 399.8 ± 0.5 eV region, corresponds to the N-H bonds referent to -NH_2 groups free on the surface, indicating silanes covalently bonded on the surface. The peak located at higher binding energies, in the region of 401.0–402.5 eV, may be associated with different protonated amine [45–47].

SEM images revealed crust-like structures over the surfaces treated with thin film (Tf), presenting clusters in samples with the application of APTMS Tf-A, both for Y-TZP and Y-PSZ zirconia (Fig. 6). As for the manual nanotube groups (MNt), large clusters are seen over the surfaces of both zirconia types, with few differences between silanized and non-silanized samples. The groups with vacuum nanotubes (VNt) presented fewer clusters than MNt groups and structures of the same size as manual application groups. All samples differed from control samples, which exhibited smooth surfaces.

Regarding μSBS, significant differences were observed for type of zirconia ($p < 0.0001$) and surface treatment ($p < 0.0001$). A significant interaction effect between these variables was also present ($p < 0.0001$). According to Table 3, the highest mean μSBS values were found for Y-TZP treated with vacuum nanotubes (VNt) while samples treated with APTMS exhibited the lowest mean values. In general, Y-TZP zirconia groups presented higher mean values than Y-PSZ even for control treatments. The groups treated with thin film presented similar results to

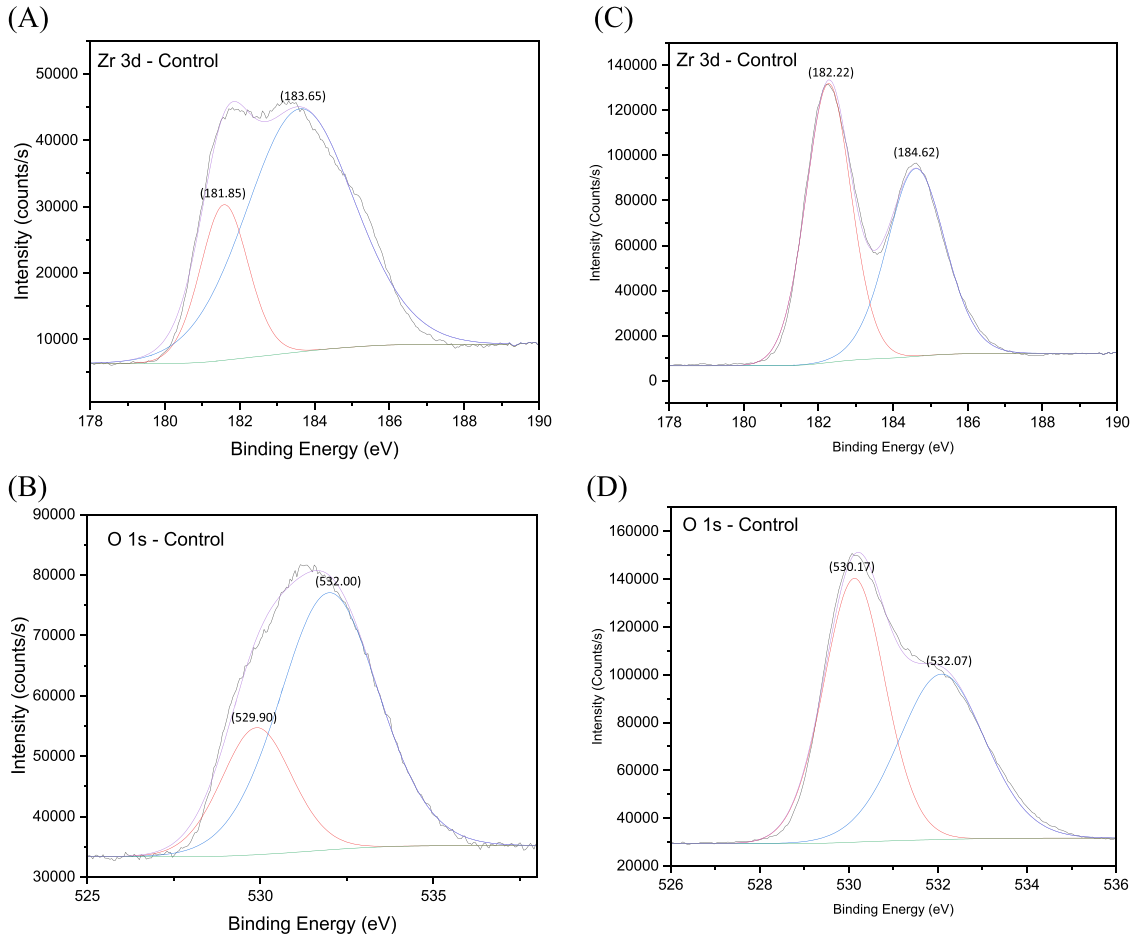

Fig. 3. XPS high-resolution spectra for the elements Zr 3d and O 1 s present on Y-TZP and Y-PSZ control groups.

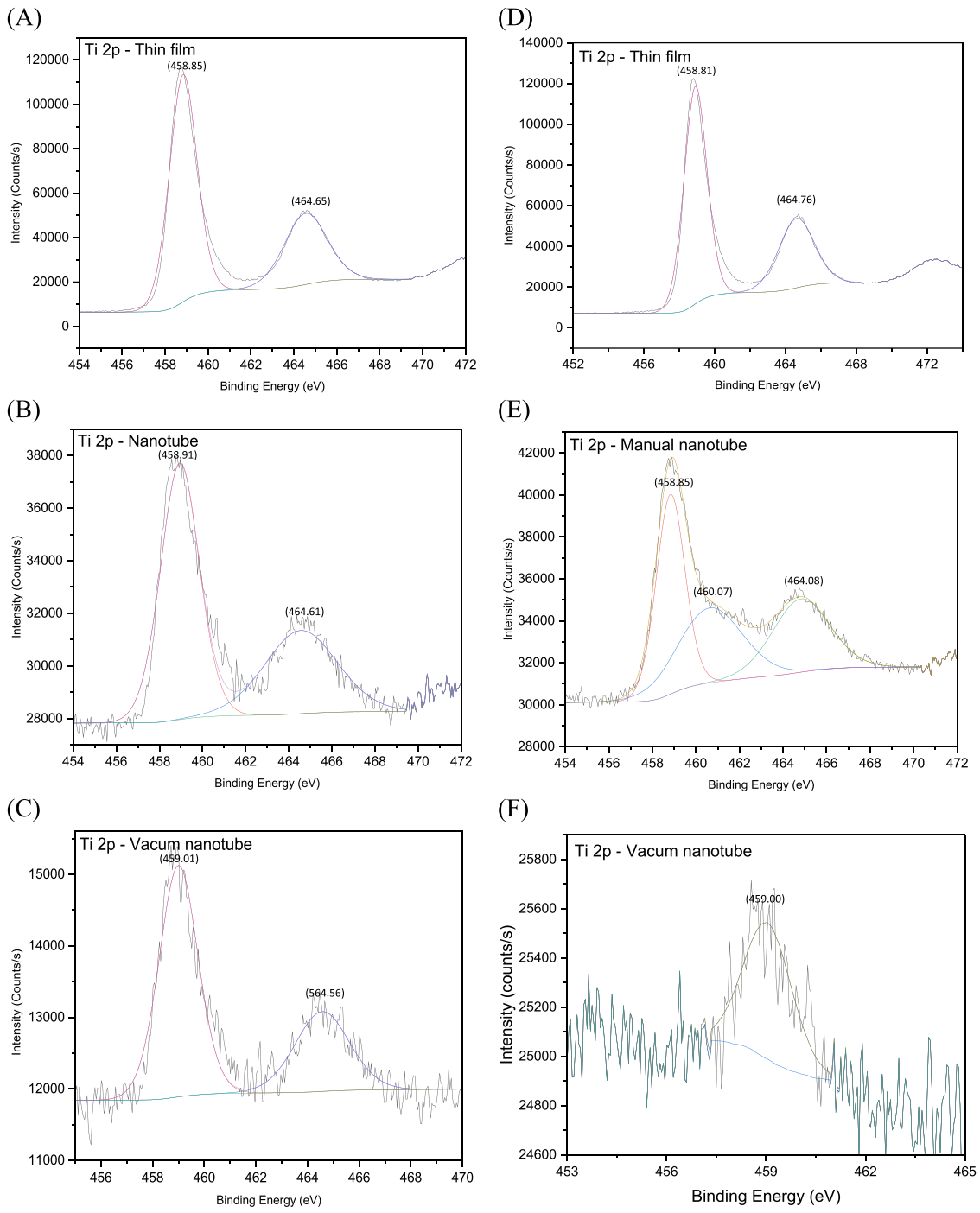

Fig. 4. XPS high-resolution spectra for the element Ti 2p present on groups (A) T-Tf, (B) T-MNt, (C) T-VNt, (D) P-Tf, (E) P-MNt, and (F) P-VNt. Obtained through CasaXPS (Casa Software Ltd) and Origin (EA).

the control groups and to the highest values obtained for VNt. Additionally, APTMS silane provided μSBS similar to the control only in association with thin film surface treatment. The mode of failure analysis revealed predominant mixed failures for thin film treatments, nanotubes without APTMS and for the control (Fig. 7). Regarding nanotubes treated with nanotubes with APTMS, failures were predominantly adhesive between the zirconia and the cement.

4. Discussion

Bonding to zirconia materials has become the aim of numerous studies. Although it presents excellent mechanical properties, its high chemical stability impairs bonding of non-retentive restorations and prosthesis. In the present study, the null hypotheses were partially accepted, the null hypothesis regarding (1) the surface modification was rejected and the hypotheses referring difference between (2) zirconia materials and (3) surface treatments were accepted. The experimental surface treatments revealed the modification of both Y-TZP and Y-PSZ surfaces, promoting the formation of covalent bonds and providing adhesion to resin-based materials, bond strength evaluation showed that TiO_2 thin film application resulted in values comparable to conventional protocols of sandblasting. Thus, main reasons for differences between surface treatments are related to manual and vacuum with APTMS that did not provide good results. Results showed APTMS was effective in

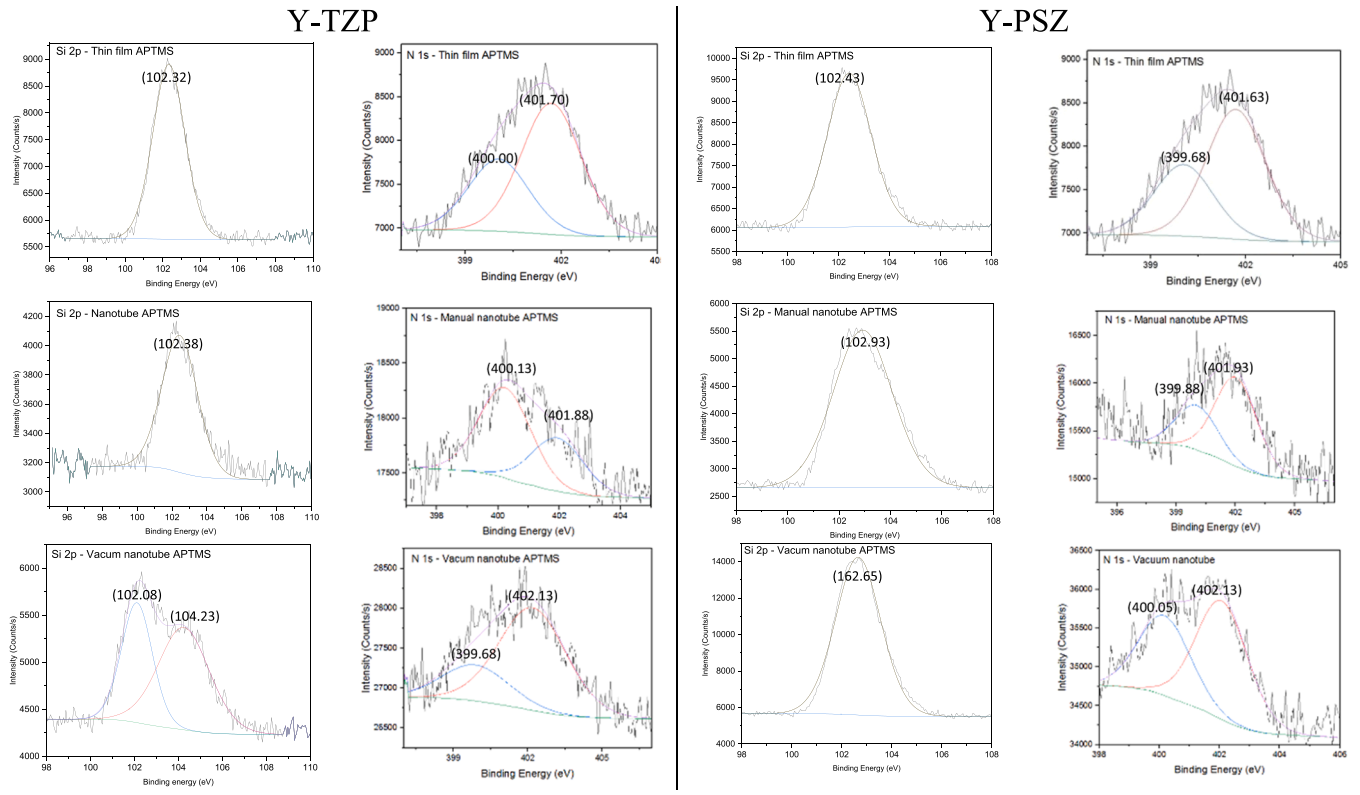

Fig. 5. XPS high-resolution spectra for the elements Si 2p and N 1 s for groups functionalized with APTMS.

functionalizing the surface, albeit leading to pre-test failures in association with certain surface treatments. This suggests other functionalizing materials should be evaluated.

The formation of thin films over ceramic and metallic substrates is an alternative to modify surfaces and provide several advantages. The deposition of thin films of TiO_2 have been previously reported and exhibited a favorable biologic response over implant metal surfaces, increasing adhesion of bone [31,48]. The explanation for such behavior may be related to the increase of hydroxyl groups over the surface, which increase the reactivity with other molecules to form covalent bonds [31]. Likewise, the formation of TiO_2 thin films over zirconia surfaces is expected to improve bonding through such mechanisms. The present study validated the TiO_2 deposition through XPS, showing the signals corresponding to TiO_2, Ti 3d and O 1 s in Figs. 1 and 2. Ti 2p high resolution spectra for T-Tf, T-MNt, T-VNt, P-Tf, P-MNt, P-VNt are displayed in Fig. 4. Ti 2p spectrum presents two spin orbit coupling contributions, Ti 2p1/2 and Ti 2p3/2 in 458.8± 0.2 eV and 464.6 ±0.2 eV, which are consistent to Ti^{4+} in TiO_2 bond (Ti-O bond) [42–44]. These peaks are related to Ti-O bonds in the oxide and Ti-OH on the surface, which are consistent with previous studies involving the interaction between ZrO_2 and TiO_2 [42–44].

Furthermore, changes in displacement (0.2 eV) and intensity are observed at Zr 3d5/2 and Zr 3d3/2 peaks (Fig. 3). The low displacement of the Zr3d peaks demonstrates that there were no significant changes in the binding energy, indicating that the chemical state of Zr in the materials does not change. Therefore, the alteration would be related to the electronic distribution close to the Zr-O bond, with the presence of more species with different chemical characteristics, indicating the formation of Zr-O-Ti bonds [49]. The intensity is associated with the Zr/Ti ratio on the material. The deconvolution of the O 1 s spectra after TiO_2 deposition (Fig. 4) presents three binding energies contributions at 530.0±0.2, 531.20±0.2 eV and 532.6±0.5 eV associated with Ti-O/Zr-O, Ti-O-Zr- and Ti-OH/Zr-OH interactions, confirming an interaction between ZrO_2 and TiO_2 in the synthesized materials. P-VNt shows two contributions in O 1 s (see supplemental materials) high-resolution, 530.01±0.2 eV and 531.9 ±0.2 eV, referring to Ti-O/Zr-O and Ti-O-Zr-/ Ti-OH/Zr-OH bonds, respectively. The peaks at higher binding energies may be associated with the adsorption of water on the surface.

A promising finding of the present study was the ability to deposit a thin film of TiO_2 over the surface of zirconia, rendering satisfactory results of bonding compared to the positive controls. Such a technique has been employed in several areas of dentistry and industry with different techniques of application [32,33]. SEM images showed a uniform layer formation and certain cluster formations for thin film groups. As a result, SBS test corroborates the presence of such structure, indicating a satisfactory bond strength compared to the controls. Such results are of great importance, considering Y-PSZ presents greater content o cubic phase crystals, impairing its phase transformation and reducing its resistance after a sandblasting protocol [16]. Another advantage of using thin films is related to the experimental functionalization, considering it presented a satisfactory SBS when combined with APTMS, as opposed to surfaces covered with nanotubes. The favorable combination of thin film with APTMS agrees with previous studies that demonstrated effective functionalization [31,50].

High resolution XPS data of Si 2p and N 1 s (Fig. 5) binding energies are important in determining the type of interaction and/or molecular bond formed between silane and substrate [45,51]. Si 2p spectrum shows a peak in the region of 102.40 eV, referring to Si-O-Ti/Si-O- bonds. T-VNt-A presented Si 2p with two deconvolution peaks in the regions of 102.10 eV and 104.2 eV associated with Si-O groups and SiO_2, respectively. The presence of SiO_2 may be associated with the intramolecular interaction and/or intermolecular bonds between neighboring APTMS molecules (−O–Si–O–Si–) in the adsorption layer. Additionally, N 1 s peak at low binding energy, 399.8 ± 0.5 eV region (Fig. 5), corresponds to the N-H bonds referent to -NH_2 groups free on the surface, indicating silane covalently bonded to the surface. The peak located at higher binding energies, in the region of 401.0–402.5 eV, may be associated with different protonated amine: (I) protonated NH_2 group

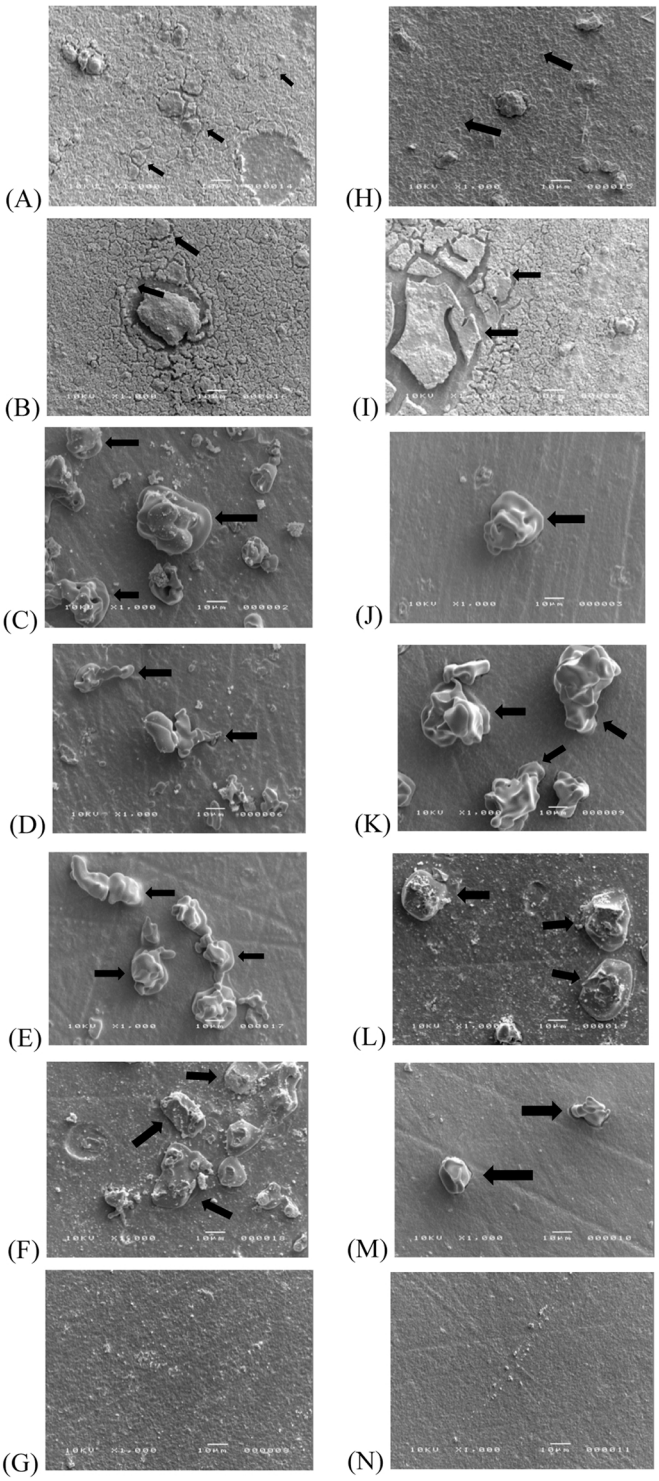

Fig. 6. - SEM images showing Y-TZP treated with T-Nf-A (A), T-Nf (B), T-MNt-A (C), T-MNt (D), T-VNt-A (E), T-VNt (F), T-C (G), and Y-PSZ treated with P-Nf-A (H), P-Nf (I), P-MNt-A (J), P-MNt (K), P-VNt-A (L), P-VNt (M), P-C (N), obtained at 1000x magnificatio.

($-NH_3^+$) associated with the zwitterionic amine formation, or protonated by the solvent [45–47]; (II) to amine groups protonated by interactions with other free silanes, and/ or (III) amino groups forming inter and intramolecular hydrogen bonds with the hydroxyl group of Titanium/Zirconium surface [45–47].

Although APTMS was used to functionalize TiO_2 surfaces in previous studies [23,31,50], poor results of bond strength were observed for

Table 3
Results of microshear bond strength in MPa.

Material	Surface treatment	Shear bond strength (MPa)	Sample losses (%)
Y-TZP	TiO_2 thin film with APTMS	10.01 (4.54)^{bcda}	10
	TiO_2 thin film*	16.65 (7.50)^{abaa}	0
	Manual nanotubes with APTMS	00.03 (0.07)^{eaaa}	80
	Manual nanotubes*	14.83 (9.09)^{abca}	10
	Vacuum nanotubes with APTMS	00.13 (0.23)^{eaaa}	70
	Vacuum nanotubes*	19.28 (4.88)^{aaaa}	10
	Control**	14.07 (9.59)^{abca}	0
Y-PSZ	TiO_2 thin film with APTMS	11.66 (4.78)^{abcd}	10
	TiO_2 thin film*	11.57 (4.95)^{abcd}	0
	Manual nanotubes with APTMS	00.88 (1.26)^{eaaa}	40
	Manual nanotubes*	07.37 (3.44)^{cdea}	0
	Vacuum nanotubes with APTMS	00.04 (0.04)^{eaaa}	40
	Vacuum nanotubes*	05.58 (2.71)^{deaa}	0
	Control**	10.16 (5.96)^{bcda}	0

Different superscript letters indicate significant differences ($p < 0.05$).
*Groups in which Monobond-N was applied.
** Groups in which Al2O3 sandblast was done and Monobond-N was applied.

groups treated with nanotubes and APTMS. The structure of such molecule consists of a silicon atom in the middle, three methanol groups to one side, which would form alcoxi groups with hydroxyl of the surfaces [31], and an amine group after a short carbon chain to the other side, which interacts with the resin cement. For this reason, the poor adhesion of nanotube treated surfaces might be related to the scarcity of hydroxyl groups in these surfaces compared to the thin film, impairing the formation of enough alcoxi groups for sufficient bonding. Additionally, N 1 s high resolution provides contributions higher than 400 eV, which correspond to NH_3 groups originated from interactions that occur though hydrogen bonds [46]. Hydrogen bonds are considered much weaker when compared to intramolecular covalent bonds [52]. For future investigations, adoption of an experimental silane with a methacrylate group associated to a photoinitiator system may be beneficial, considering it would break carbon double bonds of the silane and the resin cement methacrylates to form covalent bonds. In this sense, 3-(trimethoxysilyl)propyl methacrylate (TSMPM) is a similar molecule to the silane APTMS, presenting methanol groups to one side to ensure bonding to hydroxyl groups present in the surface and a methacrylate functional group to the other side that could present covalent bond with the methacrylates of resin-based materials [50].

The choice of an experimental silane coupling agent intended to standardize a known structure that had been previously tested for films [31] and nanotubes [50], contrary to commercial agents of unknown composition. Commercial products were only employed during cementation for shear bond strength by means of characterizing unfunctionalized experimental methodologies. The choice for the commercial resin cement Multilink N is appropriate for zirconia materials, however such product does not account for 10-methacryloyloxy-decyl-dihydrogen--phosphate (10-MDP) in its composition, which present strong interactions with zirconia through ionic and hydrogen bond [53,54]. As regards the protocol of cementation, the cementation of resin composite cylinders for μSBS followed previous studies that intended to simulate the light attenuation of positioning the light through the ceramic as in a clinical scenario [23,38]. It is known that the opacity of ceramic materials affects the polymerization properties of resin cements depending on the thickness of the cement line [55–57]. Thus, an alternative to provide an adequate cementation was to light-cure a small layer of resin cement rather than building a 1 mm cement cylinder [38].

Despite its limitations, the present study was able to propose a novel technique for surface treatment of zirconia surfaces as an alternative to

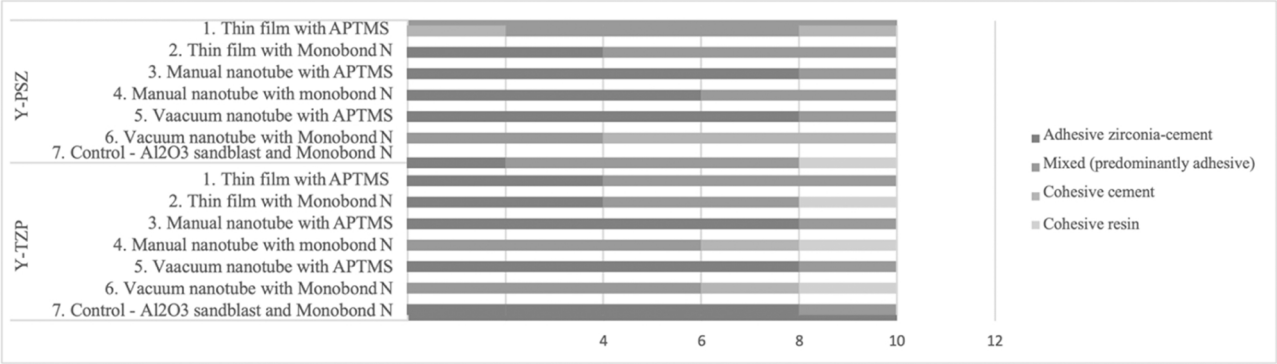

Fig. 7. Mode of failure of samples submitted to SBS.

conventional airborne abrasion, providing comparable bonding and avoiding the risk crack initiation, which was previously reported on other studeis [15,16,58]. At the same time, some environmental issues of using airborne particles should not be overlooked, since sandblasting may be conducted by either the lab technician, who usually uses proper protective chambers, or the dentist inside de dental office using hand-held devices. However, on either situation the risks of inhaling such particles that may stay suspended on the air still exists. The costs for producing TiO_2 nanotubes by hydrothermal systems is low and the technique do not demand expensive/sophisticated equipment. Although airborne-particle abrasion is a simple and cost-effective method which is already well-accepted by clinicians and laboratories, potential benefits of exclusively chemical bonding should be further evaluated in an attempt to increase the longevity of zirconia restorations. This is especially interesting considering the new generations of translucent zirconia that may be further processed for obtaining ultrathin minimally invasive dental restorations such as “contact lens” veneers and “tabletop” overlays. Additionally, the results obtained from the present in vitro do not account for external factors of the clinical settings such as the masticatory forces, degrading components of saliva and pH variations from the diet, despite of the ageing protocol adopted for simulating temperature variations according to previous in vitro protocols [59,60]. Other studies addressing different protocols for functionalizing zirconia surfaces after TiO_2 application should be conducted, since in the present study only two functionalization materials (i.e. Monobond-N and APTMS) were evaluated.

5. Conclusions

Surface treatments with TiO_2 nanostructures were effective in modifying the surface of both zirconia materials, Y-TZP and Y-PSZ. Experimental treatments yielded strong covalent bonds, which were demonstrated by the presence of XPS signals representative of Ti-O-Si and Zr-O-Si bonds. Alterations in surface topology were verified by MEV images of the surface, showing nanostructures in the form of film and clusters. Shear bond strength of experimental surface treatments was comparable to conventional sandblasting protocols. Within the limitations of this study, surface treatments with TiO_2 nanostructures figure as an alternative method of modifying zirconia surface to obtain satisfactory adhesion to resin-based luting agents. In addition, the experimental protocol dispenses the use of air-borne particle abrasion, which provide adhesion at the expenses of microcracks on the ceramic surface. Future studies addressing new methods of experimental surface functionalization and their interaction with dental adhesives containing functional monomers could be conducted.

Declaration of Competing Interest

The authors declare the following financial interests/personal relationships which may be considered as potential competing interests. Adilson Yoshio Furuse reports financial support was provided by State of Sao Paulo Research Foundation. Constantino Fernandes Neto reports financial support was provided by State of Sao Paulo Research Foundation. Constantino Fernandes Neto reports financial support was provided by Coordination of Higher Education Personnel Improvement. Constantino Fernandes Neto reports financial support was provided by National Council for Scientific and Technological Development.

Acknowlegdments

Study supported in part by Coordenação de Aperfeiçoamento Pessoal de Nível Superior – Brazil (CAPES) – Finance Code 0001, Conselho Nacional de Desenvolvimento Científico e Tecnológico - Brazil (CNPq) under the finance code 133546/2019-5, and Fundação de Amparo à Pesquisa do Estado de São Paulo (FAPESP) under the finance codes 2019/16816-6 and 2019/05427-9.

Appendix A. Supporting information

Supplementary data associated with this article can be found in the online version at doi:10.1016/j.nxnano.2024.100103.

References

[1] A.N. Cavalcanti, R.M. Foxton, T.F. Watson, M.T. Oliveira, M. Giannini, G. M. Marchi, Y-TZP ceramics: key concepts for clinical application, Oper. Dent. 34 (2009) 344–351.
[2] S.R. Datla, R.K. Alla, V.R. Alluri, J. Babu, A. Konakanchi, Dental ceramics: part II – Recent advances in dental ceramics, J. Eng. Mater. Technol. 3 (2015) 19–26.
[3] Y. Zhang, B.R. Lawn, Novel Zirconia Materials in Dentistry, J. Dent. Res 97 (2018) 140–147.
[4] R.R. Seghi, D.D.R. Leyva, Biomaterials: ceramic and adhesive technologies, Dent. Clin. North Am. 63 (2019) 233–248.
[5] T. Derand, M. Molin, K. Kvam, Bond strength of composite luting cement to zirconia ceramic surfaces, Dent. Mater. 21 (2005) 1158–1162.
[6] M. Ozcan, S. Kerkdijk, L.F. Valandro, Comparison of resin cement adhesion to Y-TZP ceramic following manufacturers’ instructions of the cements only, Clin. Oral. Invest. 12 (2008) 279–282.
[7] D.M. Qeblawi, C.A. Munoz, J.D. Brewer, E.A., Jr Monaco, The effect of zirconia surface treatment on flexural strength and shear bond strength to a resin cement, J. Prosthet. Dent. 103 (2010) 210–220.
[8] F.O. Abi-Rached, S.B. Martins, A.A. Almeida-Junior, G.L. Adabo, M.S. Goes, R. G. Fonseca, Air abrasion before and/or after zirconia sintering: surface characterization, flexural strength, and resin cement bond strength, Oper. Dent. 40 (2015) E66–E75.
[9] P. Jevnikar, K. Krnel, A. Kocjan, N. Funduk, T. Kosmac, The effect of nano-structured alumina coating on resin-bond strength to zirconia ceramics, Dent. Mater. 26 (2010) 688–696.
[10] P. Baldissara, M. Querze, C. Monaco, R. Scotti, R.G. Fonseca, Efficacy of surface treatments on the bond strength of resin cements to two brands of zirconia ceramic, J. Adhes. Dent. 15 (2013) 259–267.
[11] M. Ozcan, M. Bernasconi, Adhesion to zirconia used for dental restorations: a systematic review and meta-analysis, J. Adhes. Dent. 17 (2015) 7–26.
[12] N. Demir, M.G. Subasi, A.N. Ozturk, Surface roughness and morphologic changes of zirconia following different surface treatments, Photo Laser Surg. 30 (2012) 339–345.

[13] D. Scaminaci Russo, F. Cinelli, C. Sarti, L. Giachetti, Adhesion to zirconia: a systematic review of current conditioning methods and bonding materials, Dent. J. 7 (2019) 74.
[14] R. Comino-Garayoa, J. Peláez, C. Tobar, V. Rodríguez, M.J. Suárez, Adhesion to Zirconia: a systematic review of surface pretreatments and resin cements, Materials 14 (2021) 2751.
[15] B.R. Lawn, Y. Deng, I.K. Lloyd, M. Janal, E. Rekow, V. Thompson, Materials design of ceramic-based layer structures for crowns, J. Dent. Res 81 (2002) 433–438.
[16] B. Chen, Y. Yan, H. Xie, H. Meng, H. Zhang, C. Chen, Effects of tribochemical silica coating and alumina-particle air abrasion on 3Y-TZP and 5Y-TZP: evaluation of surface hardness, roughness, bonding, and phase transformation, J. Adhes. Dent. 22 (2020) 373–382.
[17] A.F. Dos Santos, F. Sandes de Lucena, A.F. Sanches Borges, P.N. Lisboa-Filho, A. Y. Furuse, Incorporation of TiO_2 nanotubes in a polycrystalline zirconia: Synthesis of nanotubes, surface characterization, and bond strength, J. Prosthet. Dent. 120 (2018) 589–595.
[18] A. Reis, G.F. Ramos, T.M.B. Campos, P. Prado, G. Vasconcelos, A.L.S. Borges, et al., The performance of sol-gel silica coated Y-TZP for veneered and monolithic dental restorations, J. Mech. Behav. Biomed. Mater. 90 (2019) 515–522.
[19] J.A. Rodríguez, M.Synthesis Fernández-García, properties, and applications of oxide nanomaterials, John Wiley & Sons, Hoboken, 2007.
[20] L.B. Arruda, C.M. Santos, M.O. Orlandi, W.H. Schreiner, Lisboa PN. Formation and evolution of TiO_2 nanotubes in alkaline synthesis, Ceram. Int 41 (2015) 2884–2891.
[21] T. Shimizu, S. Fujibayashi, S. Yamaguchi, K. Yamamoto, B. Otsuki, M. Takemoto, et al., Bioactivity of sol–gel-derived TiO2 coating on polyetheretherketone: in vitro and in vivo studies, Acta Biomater. 35 (2016) 305–317.
[22] P. Silva-Bermudez, S. Rodil, An overview of protein adsorption on metal oxide coatings for biomedical implants, Surf. Coat. Technol. 233 (2013) 147–158.
[23] F.N. Mezarina-Kanashiro, E.S. Bronze-Uhle, F.A.P. Rizzante, P.N. Lisboa-Filho, A.F. S. Borges, A.Y. Furuse, A new technique for incorporation of TiO_2 nanotubes on a pre-sintered Y-TZP and its effect on bond strength as compared to conventional air-borne particle abrasion and silicatization TiO_2 nanotubes application on pre-sintered Y-TZP, Dent. Mater. 38 (2022) e220–e230.
[24] K. Lee, A. Mazare, P. Schmuki, One-dimensional titanium dioxide nanomaterials: nanotubes, Chem. Rev. 114 (19) (2014) 9385–9454.
[25] E. Ovodok, H. Maltanava, S. Poznyak, M. Ivanovskaya, A. Kudlash, N. Scharnagl, et al., Sol-gel template synthesis of mesoporous carbon-doped TiO2 with photocatalytic activity under visible light, Mater. Today Proc. 5 (2018) 17422–17430.
[26] F.G. Oliveira, A.R. Ribeiro, G. Perez, B.S. Archanjo, C.P. Gouvea, J.R. Araújo, et al., Understanding growth mechanisms and tribocorrosion behaviour of porous TiO2 anodic films containing calcium, phosphorous and magnesium, Appl. Surf. Sci. 341 (2015) 1–12.
[27] M. Lilja, J. Forsgren, K. Welch, M. Åstrand, H. Engqvist, M. Strømme, Photocatalytic and antimicrobial properties of surgical implant coatings of titanium dioxide deposited though cathodic arc evaporation, Biotechnol. Lett. 34 (2012) 2299–2305.
[28] M. Machida, K. Norimoto, T. Kimura, Antibacterial activity of photocatalytic titanium dioxide thin films with photodeposited silver on the surface of sanitary ware, J. Am. Ceram. Soc. 88 (2005) 95–100.
[29] X. Wang, Z. Li, J. Shi, Y. Yu, One-dimensional titanium dioxide nanomaterials: nanowires, nanorods, and nanobelts, Chem. Rev. 114 (19) (2014) 9346–9384.
[30] A. Fujishima, X. Zhang, D.A. Tryk, TiO2 photocatalysis and related surface phenomena, Surf. Sci. Rep. 63 (2008) 515–582.
[31] L.D. Trino, E.S. Bronze-Uhle, A. George, M.T. Mathew, Lisboa PN. surface physicochemical and structural analysis of functionalized titanium dioxide films, Colloid Surf. A Physicochem Eng. Asp. 546 (2018) 168–178.
[32] S. Cao, Y. Wang, L. Cao, Y. Wang, B. Lin, W. Lan, et al., Preparation and antimicrobial assay of ceramic brackets coated with TiO2 thin films, Korean J. Orthod. 46 (2016) 146–154.
[33] D. Macwan, P.N. Dave, S. Chaturvedi, A review on nano-TiO 2 sol–gel type syntheses and its applications, J. Mater. Sci. 46 (2011) 3669–3686.
[34] A.Y. Fadeev, R. Helmy, S. Marcinko, Self-assembled monolayers of organosilicon hydrides supported on titanium, zirconium, and hafnium dioxides, Langmuir 18 (20) (2002) 7521–7529.
[35] A. Hafezeqoran, R. Koodaryan, Double-layer surface modification of polyamide denture base material by functionalized sol-gel based silica for adhesion improvement, J. Prosthodont 28 (2019) 701–708.
[36] E.S. Bronze-Uhle, L.F. Dias, L.D. Trino, A.A. Matos, R.C. de Oliveira, P.N. Lisboa-Filho, Physicochemical bisphosphonate immobilization on titanium dioxide thin films surface by UV radiation for bio-application, Surf. Coat. Technol. 357 (2019) 36–47.
[37] N. Tabet, M. Faiz, A. Al-Oteibi, XPS study of nitrogen-implanted ZnO thin films obtained by DC-Magnetron reactive plasma, J. Electron Spectros Relat. Phenom. 163 (1-3) (2008) 15–18.
[38] C. Fernandes Neto, M.H. Narimatsu, P.H. Magão, R.M. da Costa, C.S. Pfeifer, A. Y. Furuse, Physical-chemical characterization and bond strength to zirconia of dental adhesives with different monomer mixtures and photoinitiator systems light-activated with poly and monowave devices, Biomater. Invest. Dent. 9 (2022) 20–32.
[39] C. Belver, J. Bedia, J. Rodriguez, Zr-doped TiO2 supported on delaminated clay materials for solar photocatalytic treatment of emerging pollutants, J. Hazard Mater. 322 (2017) 233–242.
[40] S. Vempati, F. Kayaci-Senirmak, C. Ozgit-Akgun, N. Biyikli, T. Uyar, Amorphous to tetragonal zirconia nanostructures and evolution of valence and core regions, J. Phys. Chem. C. Nanomater Interfaces 119 (40) (2015) 23268–23273.
[41] J. Bae, S.-S. Park, B. Mun, S. Park, E. Hwang, J. Kim, et al., Surface modification of yttria-stabilized-zirconia thin films under various oxygen partial pressures, Thin Solid Films 520 (17) (2012) 5826–5831.
[42] B.M. Reddy, B. Chowdhury, P.G. Smirniotis, An XPS study of the dispersion of MoO3 on TiO2–ZrO2, TiO2–SiO2, TiO2–Al2O3, SiO2–ZrO2, and SiO2–TiO2–ZrO2 mixed oxides, Appl. Catal. 211 (2001) 19–30.
[43] Y. Gnatyuk, N. Smirnova, O. Korduban, A. Eremenko, Effect of zirconium incorporation on the stabilization of TiO_2 mesoporous structure, Surf. Interface Anal. 42 (6-7) (2010) 1276–1280.
[44] M. Andrulevičius, S. Tamulevičius, Y. Gnatyuk, N. Vityuk, N. Smirnova, A. Eremenko, XPS investigation of TiO2/ZrO2/SiO2 films modified with Ag/Au nanoparticles, Medziagotyra 14 (2008) 8–14.
[45] D. Meroni, L. Lo Presti, G. Di Liberto, M. Ceotto, R.G. Acres, K.C. Prince, et al., A close look at the structure of the TiO2-APTES interface in hybrid nanomaterials and its degradation pathway: an experimental and theoretical study, J. Phys. Chem. C. Nanomater Interfaces 121 (2017) 430–440.
[46] N. Graf, E. Yegen, T. Gross, A. Lippitz, W. Weigel, S. Krakert, et al., XPS and NEXAFS studies of aliphatic and aromatic amine species on functionalized surfaces, Surf. Sci. 603 (18) (2009) 2849–2860.
[47] Y.-Y. Song, H. Hildebrand, P. Schmuki, Optimized monolayer grafting of 3-aminopropyltriethoxysilane onto amorphous, anatase and rutile TiO2, Surf. Sci. 604 (3-4) (2010) 346–353.
[48] H.N. Pantaroto, J.M. Cordeiro, L.T. Pereira, A.B. de Almeida, F.H.N. Junior, E. C. Rangel, et al., Sputtered crystalline TiO2 film drives improved surface properties of titanium-based biomedical implants, Mater. Sci. Eng. C. Mater. Biol. Appl. 119 (2021) 111638.
[49] A. Juma, I.O. Acik, A. Oluwabi, A. Mere, V. Mikli, M. Danilson, et al., Zirconium doped TiO2 thin films deposited by chemical spray pyrolysis, Appl. Surf. Sci. 387 (2016) 539–545.
[50] G.M. Guimarães, E.S. Bronze-Uhle, P.N. Lisboa-Filho, A.P.P. Fugolin, A.F.S. Borges, C.C. Gonzaga, et al., Effect of the addition of functionalized TiO2 nanotubes and nanoparticles on properties of experimental resin composites, Dent. Mater. 36 (2020) 1544–1556.
[51] R.G. Acres, A.V. Ellis, J. Alvino, C.E. Lenahan, D.A. Khodakov, G.F. Metha, et al., Molecular structure of 3-aminopropyltriethoxysilane layers formed on silanol-terminated silicon surfaces, J. Phys. Chem. C. Nanomater Interfaces 116 (2012) 6289–6297.
[52] A. Gavezzotti, Comparing the strength of covalent bonds, intermolecular hydrogen bonds and other intermolecular interactions for organic molecules: X-ray diffraction data and quantum chemical calculations, N. J. Chem. 40 (2016) 6848–6853.
[53] N. Nagaoka, K. Yoshihara, V.P. Feitosa, Y. Tamada, M. Irie, Y. Yoshida, et al., Chemical interaction mechanism of 10-MDP with zirconia, Sci. Rep. 7 (2017) 45563.
[54] R.B.W. Lima, S.C. Barreto, N.M. Alfrisany, T.S. Porto, G.M. De Souza, M.F. De Goes, Effect of silane and MDP-based primers on physico-chemical properties of zirconia and its bond strength to resin cement, Dent. Mater. 35 (2019) 1557–1567.
[55] A.Y. Furuse, L.O.C. Santana, F.A.P. Rizzante, S.K. Ishikiriama, J.F. Bombonatti, G. M. Correr, et al., Delayed Light Activation Improves Color Stability of Dual-Cured Resin Cements, J. Prosthodont 27 (2018) 449–455.
[56] R.R. Pacheco, A.O. Carvalho, C.B. Andre, A.P.A. Ayres, R.B.C. de Sa, T.M. Dias, et al., Effect of indirect restorative material and thickness on light transmission at different wavelengths, J. Prosthodont Res 63 (2019) 232–238.
[57] B. Yang, Q. Huang, B. Holmes, J. Guo, Y. Li, Y. Heo, et al., Influence of curing modes on the degree of conversion and mechanical parameters of dual-cured luting agents, J. Prosthodont Res 64 (2020) 137–144.
[58] E.A. McLaren, N. Lawson, J. Choi, J. Kang, C. Trujillo, New high-translucent cubic-phase-containing zirconia: clinical and laboratory considerations and the effect of air abrasion on strength, Compend Contin. Educ. Dent. 38 (2017 Jun) 13–16.
[59] D.M.D. Moura, A.B. do Nascimento Januário, A.M.M. de Araújo, A.M.D.O. dal Piva, M. Özcan, M.A. Bottino, et al., Effect of primer-cement system with different functional phosphate monomers on the adhesion of zirconia to dentin. J. Mech. Behav. Biomed. Mater. 88 (2018) 69–77.
[60] A.L. Morresi, M. D'amario, M. Capogreco, R. Gatto, G. Marzo, C. D'Arcangelo, et al., Thermal cycling for restorative materials: does standardized protocol exist in laboratory testing? A literature review, J. Mech. Behav. Biomed. Mater. 29 (2014) 295–308.